Zeb1 represses TCR signaling, promotes the proliferation of T cell progenitors and is essential for NK1.1+ T cell development

Jiang Zhang, Mélanie Wencker, Quentin Marliac, Aurore Berton, Uzma Hasan, Raphaël Schneider, Daphné Laubreton, Dylan E Cherrier, Anne-Laure Mathieu, Amaury Rey, et al.

Zeb1 represses TCR signaling, promotes proliferation in T cell progenitors and is essential for NK1.1^{+} T cell development

Jiang Zhang[1,2,3,4,5,6], Mélanie Wencker[1,2,3,4,5], Quentin Marliac[1,2,3,4,5], Aurore Berton[1,2,3,4,5], Uzma Hasan[1,2,3,4,5], Raphaël Schneider[7], Daphné Laubreton[1,2,3,4,5], Dylan E. Cherrier[1,2,3,4,5], Anne-Laure Mathieu[1,2,3,4,5], Amaury Rey[1,2,3,4,5], Wenzheng Jiang[6], Julie Caramel[8], Laurent Genestier[8], Antoine Marçais[1,2,3,4,5], Jacqueline Marvel[1,2,3,4,5], Yad Ghavi-Helm[7], and Thierry Walzer[1,2,3,4,5]

1 CIRI, Centre International de Recherche en Infectiologie - International Center for Infectiology Research, Lyon, 69007 France.
2 Inserm, U1111, Lyon, France.
3 Ecole Normale Supérieure de Lyon, Lyon, France.
4 Université Lyon 1, Lyon, France.
5 CNRS, UMR5308, Lyon, France
6 Shanghai Key Laboratory of Regulatory Biology, School of Life Sciences, East China Normal University, Shanghai, China
7 Institut de Génomique Fonctionnelle de Lyon, CNRS UMR 5242, Ecole Normale Supérieure de Lyon, Université Claude Bernard Lyon 1, 46 allée d'Italie F-69364 Lyon, France
8 CRCL, Centre de Recherche sur le Cancer de Lyon, INSERM U1052 - CNRS UMR5286, Centre Léon Bérard, Université Claude Bernard Lyon 1, Lyon, France

Corresponding author:
Thierry Walzer (orcid.org/0000-0002-0857-8179)
Centre International de Recherche en Infectiologie (CIRI), INSERM U1111 – CNRS UMR5308, Université Lyon 1, ENS de Lyon. 21 Avenue Tony Garnier - 69365 LYON cedex 07, France. Tel +33 (0)437 28 23 73. E-mail: thierry.walzer@inserm.fr

Abstract

T cell development proceeds under the influence of a network of transcription factors (TFs). The precise role of Zeb1, a member of this network remains unclear. Here, we report that Zeb1 expression is induced early on during T cell development at the Cd4-Cd8- double negative (DN) stage 2. Zeb1 expression further augments at the Cd4+Cd8+ double positive (DP) stage before decreasing in more mature subsets. We performed an exhaustive characterization of T cells in *Cellophane* mice that bear *Zeb1* hypomorphic mutations. The Zeb1 mutation, profoundly affected all thymic subsets, specially DN2 and DP cells. Zeb1 promoted survival and proliferation in both populations in a cell-intrinsic manner. In the periphery of *Cellophane* mice, the number of conventional T cells was near normal, but invariant iNKT cells, $NK1.1^+$ γδ T cells and $Ly49^+$ Cd8 T cells were virtually absent. This suggested that Zeb1 regulates the development of unconventional T cells from DP progenitors. A transcriptomic analysis of WT and *Cellophane* DP revealed that Zeb1 regulated the expression of multiple genes involved in cell cycle and TCR signaling, possibly in cooperation with Tcf1 and Heb. Indeed, *Cellophane* DP displayed stronger signaling than WT DP upon TCR engagement in terms of calcium response, phosphorylation events and expression of early genes. Thus, Zeb1 is a key regulator of cell cycle and TCR signaling during thymic T cell development. We propose that thymocyte selection is perturbed in Zeb1-mutated mice, in a way that does not allow the survival of unconventional T cell subsets.

Introduction

T cell development occurs in the thymus and starts from immature thymocytes that are double negative (DN) for Cd4 and Cd8 expression. The DN population can be subdivided into four subsets, DN1-DN4, depending on the expression of the cell surface molecules Cd44 and Cd25 (for a review, see [1]). DN1 cells ($Cd44^{+}Cd25^{-}$) are the most immature progenitors and retain the ability to differentiate into non-T cell lineages. In DN2 cells ($Cd44^{+}Cd25^{+}$), the expression of RAG1/2 is induced, which promotes the rearrangements of gene segments encoding for TCR-β, TCR-γ, and TCR-δ subunits. In DN3 cells ($Cd44^{-}Cd25^{+}$) the TCR β-chain associates with the pre-TCR α-chain and Cd3 subunits to form the pre-TCR complex; the pre-TCR allows β-selection to occur. During β-selection, DN3 cells with productive TCRβ rearrangements receive survival and proliferative signals and mature into the DN4 ($Cd44^{-}Cd25^{-}$) stage. DN4 thymocytes then develop into $Cd4^{+}Cd8^{+}$ double-positive (DP) stages [2].

At the DP stage, a succession of events takes place and determines the fate of developing T cells; including rearrangement of the T cell antigen receptor (TCR) alpha locus, association of the αβ T cell receptor, and subsequent thymic selection. In general, high affinity interactions between the αβTCR and self-peptide-MHC complexes (pMHC) presented by different thymic cells lead to negative selection and elimination of self-reactive thymocytes while low affinity interactions result in positive selection and development of Cd4 or Cd8 single positive (SP) T cells [3–5]. In spite of this general rule, regulatory T cells (Tregs) and invariant NKT cells (iNKT) receive stronger TCR signals than conventional T cells during their development [6], as a result of selection by agonist self-antigens. iNKT cells are a subset of innate like T cells with a single invariant TCRα chain (Vα14-Jα18 in mice) and a limited repertoire of TCRβ chains (Vβ8.2, Vβ7, or Vβ2) that recognize glycolipid antigens bound to Cd1d, a non-polymorphic MHC molecule [7]. Their development includes discrete stages (stages 0-3) that can be discriminated by Cd44 and NK1.1 expression [8]. Three functionally distinct iNKT cell subsets have also been identified; iNKT1 cells express T-bet and mainly secrete IFN-γ; iNKT2 cells express Gata3 and Plzf and secrete IL-4 and IL-13; iNKT17 express Rorγt and secrete IL-17. The TCR signal strength during selection governs the development of iNKT cell subsets, with strong signals promoting iNKT2 and iNKT17 development [9,10]. A large number of molecules regulate the strength of the TCR-derived signaling cascade. TCR signal

strength can also be modulated at the transcriptional level by transcription factors (TFs) such as Sox4 [11], or at the post-transcriptional level by miR-181[12,13]. The loss of either blocks iNKT cell development. Mechanistically, miR-181a regulates the expression of multiple phosphatases and other proteins to boost TCR signaling as well as cell metabolism [12,13]. Interestingly, mice expressing a hypomorphic form of Zap70, a major TCR-proximal kinase, also have impaired developmental maturation of γδ T cells, suggesting that innate-like T cell subsets are particularly dependent on a tight regulation of TCR signal strength for their development [14].

A dense network of TFs have been shown to regulate T cell development [15]. Early commitment is dependent on Notch signals [16], which induce many TFs and maintain their expression throughout T cell development. Among those factors, the E protein family factors E2a, Tcf1 (encoded by *Tcf7*) and Heb (encoded by *Tcf12*) [17] induce the expression of TCR components and balance the survival and proliferation of thymocytes [18]. Many other TF such as Gata3, Myb, Runx1, and Bcl11b also cooperate with E proteins at different developmental stages and further establish T cell identity [15,18].

Zeb family of TFs consist of Zeb1 and Zeb2. They are best known for their role in epithelial-to-mesenchymal transition (EMT). EMT programs operate at different stages of embryonic development and are downstream of Wnt, TGF-β, Bmp, Notch, and other signaling pathways [19]. *Zeb1*$^{-/-}$ mice exhibit multiple developmental defects and die at birth [20]. In pathological settings, activation of EMT programs contributes to fibrosis and cancer metastases [21]. Zeb1 and Zeb2 are highly homologous and are characterized by two clusters of zinc fingers expressed on the protein extremities. They also contain a homeodomain, a Smad-binding domain and can interact with many other TFs [22]. Zeb1 and Zeb2 are also expressed in a tightly regulated manner in the immune system and regulate cell differentiation [23]. We and others have previously shown that Zeb2 regulated terminal NK cell [24] and effector Cd8 T cell differentiation [25,26]. Mutated mice expressing a truncated form of Zeb1, that removes the C-terminal zinc finger clusters at C727, have a small and hypocellular thymus caused by a reduction in early T-cell precursors [27]. In *Cellophane* mutant mice, a T→A mutation in the seventh exon of *Zeb1* replaces the tyrosine at position 902 with a premature stop codon [28]. The resulting mRNA encodes a truncated protein lacking the C-terminal zinc finger domain, which is

predicted to be hypomorphic. *Cellophane* homozygote mice have small hypocellular thymi with fewer DP thymocytes. However, the mechanism of Zeb1 action during T cell development, and its role in mature T cell subsets remain unclear. Here, we show that *Cellophane* homozygous mice virtually lack several peripheral T cell subsets including iNKT cells, NK1.1^{+} γδ T cells and Ly49 expressing Cd8 T cells. This specific defect in innate-like T cells is caused by a cell-intrinsic role of Zeb1 in T cell development. We show that Zeb1 expression is maximal at the DN2 and DP stages of T cell development. Furthermore Zeb1 regulates the transition to the SP stage by promoting cell proliferation, survival and repressing the expression of various molecules involved in the strength of TCR signaling. Therefore, we propose that Zeb1 is a key regulator of thymocyte selection, essential for the development and survival of innate-like T cell subsets undergoing agonist-type selection.

Results

Zeb1 is highly expressed at the DN2 and DP stages of T cell development

To study the role of Zeb1 in T cell development, we sorted thymocyte subsets and measured Zeb1 transcript levels by semi-quantitative (Q) RT-PCR (reverse transcription polymerase chain reaction). As shown in Figure 1A, Zeb1 transcript levels were low in DN1, started to increase at the DN2 stage and were maximal in DP thymocytes. This expression then decreased as T cells underwent selection and matured into either conventional T cells, or iNKT cells. Interestingly, the expression of Zeb2 was somewhat reciprocal to that of Zeb1, with high expression in early thymic progenitors (DN1 to DN4) and lowest expression in DP (Figure 1B). This pattern of expression was matched by data from the Immgen consortium [29] (Figure S1A). Thus, as seen for memory T cells [30], Zeb1 and Zeb2 have reciprocal patterns of expression in thymocytes. We used the Immgen web browser to search for co-regulated genes across different immune subsets. The E-protein Heb (encoded by *Tcf12*) was in the top 3 genes found to be co-regulated with Zeb1 (Figure S1B) [29]. Heb is well known for its important role throughout T cell development [31], and especially at the DP stage[32], further pointing to Zeb1 as a potential regulator of this developmental stage. We also analyzed the expression of Zeb1 protein in total thymocytes (80% of which are composed of DP). Zeb1 was strongly expressed in WT but not *Cellophane* thymocytes. Mutant mice only expressed reduced quantities of a truncated form of Zeb1 (Figure 1C).

Impaired development of both conventional and unconventional T cells in *Cellophane* mice

To define the impact of the *Cellophane* mutation on T cell development, we analyzed the T cell composition in the thymus, spleen and lymph nodes of *Cellophane* mice. The cell numbers in spleen, and liver were normal while the number of lymphocytes was reduced in lymph nodes (LN) (Figure 2A). As shown by previous observations [28] we also observed a strong decrease in cell numbers from thymus in *Zeb1*-mutated mice (Figure 2A). This decreased number affected all subsets defined by Cd4, Cd8, Cd44 and Cd25 expression (Figure 2B-C). The $Cd4^{+}Cd8^{+}$ DP thymocytes and DN2 populations also decreased in frequency within *Cellophane* thymocytes

(Figure 2B-C). In the LN and spleen, the percentage of Cd4 T cells, and Cd8 T cells were reduced (Figure 2D-E) and the proportion of memory-phenotype Cd44$^+$ T cells from Cd8 T cells was decreased by nearly 30% (Figure 2F).

We then investigated the development of unconventional T cell subsets. We observed a drastic decrease in the frequency and in the number of iNKT cells as well as NK1.1$^+$ γδ T cells in *Cellophane* mice compared to littermate controls (Figure 3A-D). This decrease affected all organs from *Cellophane* mice (Figure 3A-D). iNKT cells were mainly affected at stage 3 (Figure 3E). To complete our analysis, we also studied memory-phenotype Ly49$^+$ Cd8 T cells which are thought to arise "naturally" in the thymus, without antigenic experience [33]. All Ly49$^+$ Cd8 T cell populations were also strongly decreased in LN and spleen from *Cellophane* mice, both in terms of frequencies and numbers, and irrespective of the inhibitory Ly49 receptor analyzed (Ly49A, Ly49F or Ly49G2) (Figure 3F-G).

Altogether, these data confirm the important role of Zeb1 in early T cell development. We also demonstrate an essential and specific role of Zeb1 in the development of peripheral T cell subsets expressing NK cell markers such as iNKT cells, NK1.1$^+$ γδ T cells and Ly49$^+$ Cd8 T cells.

Cell intrinsic role of *Zeb1* in thymic progenitors and T cell development

Zeb1 is also required for the development and expression of non-hematopoeitic tissues and cell types [20]. To test if Zeb1 had an intrinsic role in T cell development, we generated chimeric mice by reconstituting sub-lethally irradiated Ly5a (Cd45.1) mice with the BM from *Cellophane* (Cd45.2) or "WT" Ly5a x C57BL/6 (Cd45.1/2) mice. In the thymus of chimeric mice, the frequency of DN2 and DP was strongly decreased for *Cellophane* BM-reconstituted mice compared to WT BM-reconstituted mice, while the proportion of other populations defined by Cd4 and Cd8 was increased (Figure 4A). iNKT cells and Ly49$^+$ T cell subsets were also strongly reduced in the peripheral organs of *Cellophane*→Ly5a BM chimeric mice compared to WT→Ly5a chimera indicating that *Zeb1* regulated T cell development intrinsically (Figure 4B-C). Cell numbers for all thymic T cell subsets and for peripheral iNKT cells and Ly49+ T cells were decreased in *Cellophane*→Ly5a BM chimeric mice compared to WT→Ly5a chimera (Figure S2). NK1.1$^+$ γδ T cells were not analyzed because many of them are derived from fetal precursors [34], and are not reconstituted in BM

chimera mice. To further test the role of Zeb1 in the environment of developing T cells, we also made different BM chimeric mice using WT and *Cellophane* mice as both recipients and BM donors (WT→WT, WT→*Cellophane*, *Cellophane*→WT and *Cellophane*→*Cellophane*). As shown in Figure S3A-B, the frequencies and numbers of DN and DP subsets were determined by the genotype of the BM donor and not by that of the host genotype. Similar conclusions could be reached upon examination of the frequency and number of NKT cells in the thymus and in the liver (Figure S3C).

We then generated mixed BM chimera by reconstituting lethally irradiated Ly5a mice with a 1:1 mixture of BM from *Cellophane* and Ly5a x C57BL/6 (WT) mice. Cellophane T cell progenitors had a poor competitive fitness in BM chimeric mice (Figure 4D). Indeed, the percentage of cells originating from the *Cellophane* BM progenitors was already low in DN and further decreased when transitioning between DN and DP stages (Figure 4D). In the periphery of mixed BM chimeric mice, we found that the frequency of iNKT and $Ly49^+$ Cd8 T cells was strongly reduced amongst *Cellophane* compared to WT lymphocytes (Figure 4E-F), thus revealing the role of Zeb1 in T cell development is cell-intrinsic, and not due to a defective stromal environment. Of note, we also analyzed the reconstitution of myeloid cells as control. In the spleen, on average 20% of macrophages, 25% of dendritic cells and 28% of neutrophils were of *Cellophane* origin (Figure S3D), suggesting that Zeb1 regulated the development of all hematopoietic subsets, perhaps by regulating multipotent progenitors. However, the most important effects were observed for thymocytes and peripheral T cell subsets expressing NK cell markers.

Reduced survival and proliferation of *Cellophane* DN2 and DP cells

The decreased cellularity of the *Cellophane* thymi could be due to a reduced proliferation or increased apoptosis of thymocytes. To address this point, we first compared the survival of WT and *Cellophane* thymocytes upon *ex vivo* culture. We found that *Cellophane* DN2, DN3 and DN4 had a reduced *ex vivo* viability compared to their WT counterparts (Figure 5A). Moreover, after 24 or 48 h in culture, *Cellophane* DN2, DN3, DN4 and DP were also less viable than controls (Figure 5A).

Next, we compared *in vivo* proliferation of WT and *Cellophane* thymocytes, as measured by EdU incorporation. *Cellophane* DN2 and DP proliferated less than their WT counterpart, while *Cellophane* proliferated more than WT DN3 (Figure 5B). Ki67

staining corroborated our data obtained with EdU incorporation (Figure 5C-D). As all DP cells were Ki67 positive, we reported only changes in the MFI (Figure 5D).

Thus, the *Cellophane* mutation affects both the survival and proliferation of developing DN2 and DP thymocytes, which could account for the decreased number of cells in the *Cellophane* thymi.

Zeb1 **tunes TCR signal strength**

To gain insight in the mechanism of Zeb1 function, we focused on DP as they expressed the highest level of Zeb1 among thymocytes (Figure 1A). We first compared the expression of membrane proteins involved in thymocyte selection in *Cellophane* vs WT DP cells by flow cytometry. *Cellophane* DP expressed higher levels of Cd69, Cd25, and Cd5 compared to WT thymocytes (Figure 6A). Nur77 is an early response gene expressed in T cells within hours after TCR stimulation. We observed an increase in the intracellular expression for Nur77 which correlated to TCRβ levels in *Cellophane* compared to WT DP thymocytes (Figure 6A). Of note similar levels of Cd4 and Cd8 were measured (Figure 6A).

Next, we focused our attention on thymic iNKT cell subsets. The mouse thymus is known to contain at least three iNKT subsets, ie iNKT1, iNKT2 and iNKT17 that are thought to have distinct roles in the immune response [35]. NKT1 cells correspond mainly to stage 3 NKT cells. TCR signal strength governs the development of iNKT cell subsets in the thymus, in which high signal strength is necessary for iNKT2 and iNKT17 development [9,10]. We examined iNKT cell subsets by staining for Plzf and Rorγt [36] in *Cellophane* mice vs WT mice. Results in Figure 6B show a significant increase in the representation of iNKT2 and iNKT17 and a decrease in that of iNKT1 in *Cellophane* compared to control mice. These data evocated an increase in the TCR signal from DP progenitors of iNKT cells in Cellophane mice. The change in iNKT subsets was associated with subtle changes in the TCR repertoire as assessed by measuring the frequency of Vβ8, Vβ7 and Vβ2 positive cells amongst iNKT cells of each genotype. We observed a 2-fold increase in Vβ7 usage in *Cellophane* mice (Figure 6C). This could reflect the increase in iNKT2 cells as a previous article showed that Vβ7 was more often associated with iNKT2 cells [9]. Thymic *Cellophane* iNKT cells expressed normal levels of transcription factors T-bet and Egr2 but strongly reduced levels of Cd4 (Figure 6D). Since Cd4 is

known to sustain TCR signal strength [5], the selection of Cd4 ^{low} iNKT cells in *Cellophane* mice could reflect an adaptation to overt TCR signaling in *Cellophane* DP .

We then analyzed specifically TCR signaling in developing thymocytes. We started by measuring the phosphorylation (p) level of a series of signaling proteins involved in TCR-mediated activation, either at steady-state in freshly isolated thymocytes, or following TCR engagement by crosslinking anti-Cd3 antibodies. To minimize the experimental variation, we used a barcoding strategy that allowed stimulating and then staining WT and *Cellophane* thymocytes simultaneously (see methods). Results in Figure 6E-F showed an increase in pAkt (Ser473), ribosomal protein pS6, and to a lesser extent of pErk, either at steady state or following TCR engagement in *Cellophane* DP compared to WT DP. Thus, the Mapk and PI3K/Akt pathways are more active in thymocytes undergoing selection in *Cellophane* compared to control mice. To complement this analysis, we also assessed the calcium response of DP from both genotypes in response to TCR engagement. As shown in Figure 6G-H, this response was stronger for *Cellophane* DP compared to control DP both in terms of intensity (peak) and duration (area under the curve, AUC). Thus, Zeb1 tunes signal strength downstream TCR engagement at the DP stage and *Cellophane* DP have increased TCR signaling. The latter may increase negative selection and therefore account for defective T cell development in *Cellophane* mice. We also measured preTCR signaling in DN cells following stimulation with anti-CD3 antibodies. This analysis did not reveal any difference between WT and *Cellophane* DN cells (data not shown).

Zeb1 broadly shapes transcription at the transition DP→SP to promote proliferation and repress TCR signaling

To further uncover the mechanisms of Zeb1 function during T cell development, we performed RNA-seq to compare WT and *Cellophane* DP transcriptomes. We found 538 differentially expressed genes (DEGs, p-value<0.05, Log2 Fold change>1). 204 genes were increased and 334 were down regulated in *Cellophane* DP compared to WT DP. These data reveal that Zeb1 broadly shapes the genetic program of developing thymocytes (Figure 7A and Table S1). For some of the DEGs identified, antibodies were available, and we were thus able to confirm higher expression of Foxo1, Ms4a4b, Itgb7, Ccr7 and Ccr4 in *Cellophane* compared to control DP cells

303 and reciprocally we observed lower Cd81 expression in *Cellophane* DP vs WT
304 (Figure 7B).
305 Next, we queried the Immgen database to retrieve the expression profile of the
306 Zeb1-regulated geneset (induced or repressed) across all thymocyte subsets.
307 Interestingly, genes down regulated in *Cellophane* DP (ie normally induced by Zeb1)
308 correspond to genes that are normally expressed at high levels in early T cell
309 progenitors and low levels in mature T cells (Figure 7C). Their expression level
310 normally drops at the DP to SP transition, at the time when Zeb1 is highly expressed.
311 Genes up regulated in *Cellophane* DP correspond to genes that follow the reciprocal
312 pattern of expression (Figure 7C). This pattern of expression also correlates with cell
313 proliferation and TCR responsiveness in thymocytes. Indeed, irrespective of mouse
314 genotype, SP T cells are much more responsive to TCR signaling mediated calcium
315 responses than DP, but reciprocally do not cycle as much as DP (data not shown).
316 This suggests that Zeb1 promotes cell proliferation and represses TCR signaling
317 specifically at the DP stage, presumably to ensure proper selection.
318 A functional annotation analysis of DEGs in our RNAseq analysis using
319 “Metascape” [37] highlighted the cell cycle as the most down regulated biological
320 process in *Cellophane* DP compared to control DP (Figure 7D, and Table S2),
321 confirming findings in Figure 3. Pathways linked to Ifnγ (but also type I-Ifn, Table S2),
322 antigen presentation, leukocyte differentiation and apoptosis were significantly
323 associated with genes up regulated in *Cellophane* DP compared to WT (Figure 7D).
324 Of note, a modest but significant enrichment for genes involved in the calcium
325 response was also associated with these genes, corroborating our data in Figure 6.
326 To further annotate this dataset, we also performed individual Pubmed searches,
327 looking for connections between genes up regulated in *Cellophane* DP compared to
328 control DP and “T cell activation” or “TCR signaling” or “T cell development”.
329 Interestingly this analysis showed more than 25% of the genes in the list had a
330 known role in T cell activation or TCR signaling; and 10% had a role in T cell
331 development, as defined using loss-of-function mouse strains (Table S3). Moreover,
332 we used the STRING database of physical and functional protein interactions [38] to
333 further annotate genes up or down regulated in *Cellophane* DP compared to control
334 DP. In particular, we used the Pubmed module that searches for enrichment for gene
335 lists in articles in Pubmed. This unbiased analysis showed that genes up regulated in
336 *Cellophane* DP were significantly enriched for genes involved in negative selection

[39] or T cell maturation regulated by Bcl11b [40] (Table S4), which corroborated with our manual PubMed searches.

Chromatin regions remodeled at the DP stage contain Zeb1 binding motifs

Next, we wanted to determine if Zeb1 could regulate chromatin remodeling at the DP stage of T cell development. For this, we took advantage of a recently published large-scale analysis of chromatin accessibility and gene expression across 86 immune subsets including T cell developmental stages in the thymus [41]. In this study, *in silico* predictions pointed to Zeb1 as one of the few TF whose expression correlated with modifications of chromatin accessibility during thymic T cell development, and for which the corresponding chromatin regions contained sites predicted to be bound by Zeb1. Other TFs in this category included Gata3, Tcf7, Lef1, Tcf12 and Zfp740 (Figure S4A), and especially Tcf7 and Tcf12 whose role in T cell development has been well established [32]. We retrieved open chromatin regions (OCRs) for which Zeb1 motifs were discovered in this study and whose accessibility changed during T cell development (see corresponding clusters in Figure S4B) and compared the list of corresponding genes with DEGs identified in our own study between *Cellophane* and WT DP. We found an important overlap between both lists that included many of the genes previously highlighted in our analysis (Figure 7E, p-value=1.839413e-46). Altogether, these data suggest that Zeb1 is a direct transcriptional regulator of T cell development, especially operating at the DP to SP transition to promote proliferation and ensure proper selection.

Discussion

Here, we demonstrated that Zeb1 is essential for the transition through the DN2 and DP stages of T cell development as well as for the differentiation of iNKT cells, NK1.1$^+$ γδ T cells and Ly49$^+$ Cd8 T cells. Mechanistically, Zeb1 regulates the expression of a number of genes that were notably involved in cell proliferation or in TCR signaling at the DP stage. In *Cellophane* mice, these events may perturb thymic development and selection in a way that does not allow the production of NK1.1$^+$ and Ly49$^+$ T cell subsets.

Zeb1 expression was found to increase at the DN2 stage and to be maximal at the DP stage of T cell development. Accordingly, we found a decrease in frequency of DN2 and DP thymocytes in *Cellophane* mice. This could be accounted for by a cell-intrinsic role for Zeb1 in DN2 and DP proliferation. A number of genes involved in the cell cycle were differentially expressed between WT and *Cellophane* DP as revealed by our RNAseq analysis. There is also a strong link in the literature between Zeb1 and cell proliferation in cancer. In particular, Zeb1 interacts with many TFs involved in the regulation of cell growth such as Smad TFs which is downstream of several growth factor pathways [22]. Moreover, Zeb1 is known to repress cyclin-dependent kinases during EMT [21]. However, Cdkn2c and Cdkn3 were decreased by Zeb1 in DP thymocytes, suggesting differential roles of Zeb1 in epithelial versus lymphoid cells. The decreased proliferation of DN2 and DP is expected to have important consequences on the general thymic output. Indeed, we found decreased numbers of peripheral T cells in *Cellophane* mice. However, this defect was much more pronounced for iNKT cells, NK1.1$^+$ γδ T cells and Ly49$^+$ Cd8 T cells. In particular, iNKT cells were virtually absent from the periphery. This altered development was associated with an increased TCR signaling at the DP stage, which was verified by increased basal levels of Cd5 and Nur77 but also increased mTOR activity and calcium flux upon Cd3 engagement. iNKT cells are known to receive stronger TCR signals than conventional T cells during their development [6]. Thus, increased TCR signaling in *Cellophane* DP could trigger cell death i.e. via negative selection of iNKT precursors. The increased negative selection of iNKT cells has already been shown to occur in mice in which transgenic TCR-β chain conferred high affinity for self-lipid/Cd1d complexes when randomly paired with Vα14-Jα18 rearrangements [42]. Thus, increased negative selection could impair the development of iNKT cells in *Cellophane* mice, and perhaps that of other T cell

subsets expressing NK cell markers. Indeed, strong TCR-mediated signals are also important for γδ T cell development [43,44]. In particular, NK1.1$^+$ γδ T cells have an oligoclonal TCR repertoire and accumulate in mouse models of decreased TCR signaling [45], suggesting that this subset of γδ cells can also be negatively selected. The ontogeny of Ly49$^+$ Cd8 T cells is not very well known, but our data suggest that their development and selection could share common mechanisms with that of NK1.1$^+$ T cells. How does Zeb1 regulate TCR signal strength? *Cellophane* DP thymocytes expressed higher levels of TCRβ than control DP, and this could certainly lead to higher TCR signaling. Moreover, the RNAseq analysis we performed suggested multiple connections between Zeb1 and signal transduction through the TCR. For example, multiple members of the GTPases of the IMmunityAssociated Proteins (GIMAP) family (GIMAP5 and GIMAP8) were up regulated in *Cellophane* DP. Interestingly, Gimap5 enhances calcium influx following TCR stimulation [46]. Several members of the family of four-pass membrane receptors Ms4a are also up regulated in *Cellophane* DP and could reinforce TCR signaling. Indeed, transduction of Ms4a4b into naive T cells can heighten their sensitivity to antigen through a process that could involve association with costimulatory molecules [47]. Several phosphatases and kinases are also deregulated in *Cellophane* DP and could perhaps alter TCR signaling. In particular the expression of Pyk2 (encoded by *Ptk2b*) or that of Rasgrp4, Rasl1 and Rasa3 could all contribute to higher TCR signaling via the calcium flux or the Mapk pathway.

A series of TF were also deregulated in *Cellophane* DP, with a notable up regulation of JunB, Jun, Atf6, Foxo1, Stat4 or Irf7/9. JunB and Jun are essential components of AP-1 TFs and are typically induced downstream of TCR stimulation. Similar to Nur77, they could represent surrogate markers of increased TCR signaling in *Cellophane* DP. The derepression of Foxo1 could in part account for altered T cell development as it regulates Ccr7, Cd62L and S1pr1 via Klf2 [48]. The lack of Klf2 control could perturb, perhaps accelerate, the normal migration of developing thymocytes in the medullar region where negative selection occurs. Foxo1 deletion in thymocytes was reported to decrease the number of DP thymocytes, and Foxo1 deficient peripheral T cells seem to be refractory to TCR stimulation through unknown mechanisms [49]. Moreover, up regulation of Foxo1 in *Cellophane* DP could in part explain the opposite changes in cell proliferation observed in these cells

compared to control DP, since Foxo TFs are known to promote stem cell quiescence [50] and clearly contribute to the regulation of cell division, survival and metabolism in T cells [51]. A recent study showed that the transcriptional repressor Gfi1 is important to maintain Foxo1 expression at low levels in DP thymocytes [52]. In the absence of Gfi1, there was premature expression of genes normally expressed in mature T cells and accelerated maturation of DP to SP thymocytes, largely attributable to Foxo1 de-repression. Zeb1 and Gfi1 could therefore cooperate to repress Foxo1.

There are many similarities in the phenotype of *Tcf12* deficient [53] and *Cellophane* mutant mice, in particular susceptibility of DP to cell death and impaired development of iNKT cells. Moreover, microarray data from the Immgen consortium suggest that Tcf12 and Zeb1 are strongly co-regulated and ATAC-seq data predict that they control chromatin accessibility during thymic T cell development together with Gata3, Tcf1, Lef1 and Zfp740 (Figure S4 and [41]). Altogether these data suggest a strong functional link between Zeb1 and Heb (encoded by *Tcf12*), and perhaps Tcf1, which acts in coordination with Heb [32]. The fact that Zeb1 is known to bind tandem E-box motifs, suggests a possible competition between Zeb members and E-proteins for those genes regulated by tandem E-boxes. Such a competition has been previously established at least in the context of the CD4 enhancer which is repressed by Zeb1, through a competition with Heb for E-box binding [54]. Moreover, Zfh-1 and Daugtherless, the drosophila homologs of *Zeb1* and *Tcf12,* are also known to compete for the same genomic sites [55]. The deletion of *Tcf12* and *Tcf1* in thymocytes has the opposite phenotype as *Cellophane Zeb1* mutation in terms of DP proliferation [32]. This suggests that Heb and Zeb1 could have partially antagonistic activities in the regulation of genes bearing tandem E-box elements. A competition between Zeb1 and E-proteins has already been suggested in the control of GATA3 expression in human CD4 T cells [56]. *Cellophane* mice express a truncated form of Zeb1 that is also expressed at lower levels than WT Zeb1. As the phenotype of these mice is milder than that of *Zeb1*$^{-/-}$ mice, we assumed that the *Cellophane* mutation was hypomorphic. However, we cannot exclude that *Cellophane* Zeb1 can retain some DNA binding and therefore act as a dominant negative molecule by preventing binding of E-box proteins. Further work will be needed to precisely map the interactions between Zeb TFs and E proteins. This regulatory network may also include inhibitor of differentiation genes Id2 and Id3, as these TFs bind and inactivate E-proteins, thereby regulating their function. Moreover, the deficiency in Id3 has the

same impact on NK1.1+ γδ T cells as a deficiency in TCR signaling [45], which links both events.

Zeb1 genomic region is frequently deleted in cutaneous T cell lymphomas (CTCL) [57]. These deletions are often associated with genetic mutations in components of the TCR signaling machinery (recurrent alterations in *Card11, Plcg1, Lat, Rac2, Prkcq, Cd28* and genes that encode calcium channel subunits). This observation, together with our own data showing a role for *Zeb1* in repressing TCR signaling, suggest that *Zeb1* deletion could promote lymphomagenesis by releasing TCR signaling natural brakes. Of note, a previous study proposed an essential role of IL-15 in CTCL development, and showed that IL-15 expression was depressed in patients with CTCL due to promoter hypermethylation and in the failure of Zeb1 to have access to and repress the IL-15 regulatory region [58]. However, IL-15 expression was not detected in developing thymocytes in our RNAseq analysis, excluding the possibility that the IL-15 pathway could play a role in the Zeb1 mechanism of action in T cell development. Yet, we found that the transcriptional response to different cytokines such as interferons or IL-6 was increased in *Cellophane* DP (table S2). Zeb1 may therefore normally repress the response to these cytokines, presumably to ensure proper selection. TGF-β is a known regulator of iNKT cell development [59] and that it promotes early differentiation and prevents apoptosis of developing iNKT cells. A recent study showed that Zeb1 was induced by TGF-β in conventional Cd8 T cells stimulated through the TCR and was essential for memory T cell survival and function [30]. Although we failed to detect any effect of recombinant TGF-β on *Zeb1* expression in thymocytes (data not shown), it would be interesting to address this question *in vivo* using appropriate genetic models.

In summary, Zeb1 is an essential member of the TF network that regulates T cell development and selection at the DN2 and DP stages. Furthermore, we have also shown that Zeb1 allows the development of iNKT cells and other T cell subsets expressing NK cell markers by regulation of cell cycle and TCR signaling in developing thymocytes.

494

495

Material and Methods

Mice

Mice at 8 to 24 weeks were used. Wild-type C57BL/6 mice were purchased from Charles River Laboratories (L'Arbresle). *Cellophane* mice were previously described [28], littermate mice were used as controls. This study was carried out in accordance with the French recommendations in the Guide for the ethical evaluation of experiments using laboratory animals and the European guidelines 86/609/CEE. All experimental studies were approved by the bio-ethic local committee CECCAPP. Mice were bred in the Plateau de Biologie Expérimentale de la Souris (ENS, Lyon).

Bone marrow chimeric mice

8- to 10-week-old Ly5a mice were anesthetized with ketamine/xylazine before irradiation at 9 Gray with a X-ray irradiator XRAD-320. After irradiation, they were intravenously injected with 2-5x10^6 cells collected from either wild type or mutant murine bone marrow, or a mix of both (as indicated in the figures). Immune cell reconstitution was analyzed 8 weeks post BM injection.

Flow cytometry

Single-cell suspensions of the thymus, spleen and liver were used for flow cytometry. Cell viability was measured using Annexin-V (BD Biosciences)/live-dead fixable (eBiosciences) staining. Intracellular stainings for TFs were performed using Foxp3 kit (ebioscience). Lyse/Fix and PermIII buffers (BD Biosciences) were used for intracellular staining of phosphorylated proteins. Flow cytometry was carried out on a FACS Canto, a FACS LSR II, or a FACS Fortessa (Becton-Dickinson). Data were analysed using FlowJo (Treestar). Antibodies were purchased from eBioscience, BD biosciences, R&D Systems, Beckman-Coulter, Miltenyi or Biolegend. We used the following antibodies: anti-mouse Cd3 (clone 145-2C11), anti-mouse Cd4 (clone GK1.5), anti-mouse Cd8 (clone 53-6.7), anti-mouse TCRβ (clone H57-597), anti-mouse Cd69 (clone H1.2F3), anti-mouse TCR$\gamma\delta$ (clone GL3), anti-mouse NK1.1 (clone PK136), anti-mouse Cd24 (clone M1/69), anti-mouse Cd44 (clone IM7), anti-mouse Cd27 (clone LG.7F9), anti-mouse TCRVβ2 (clone B20.6), anti-mouse TCRVβ7 (clone TR310), anti-mouse TCRVβ8.1/8.2 (clone KJ16-133), anti-mouse

Ly49A (clone A1), anti-mouse Ly49E/F (clone REA218), anti-mouse Ly49G2 (clone 4D11), anti-mouse Cd45.1 (clone A20), anti-mouse Cd45.2 (clone 104), anti-mouse Nur77 (clone 12.14), anti-mouse Ccr7 (clone 4B12), anti-mouse Cd5 (clone 53-7.3), anti-mouse Cd81 (clone Eat-2), anti-mouse Cd53 (clone OX79), anti-mouse Lpam-1 (clone DATK-32), anti-mouse Foxo1 (clone C29H4), anti-mouse Ms4a4b (clone 444008), anti-mouse Cd74 (clone In1/Cd74), anti-mouse Tbet (clone 4B10), anti-mouse Egr2 (clone erongr2), anti-mouse Plzf (clone Mags.21F7), anti-mouse Rorγt (clone AFKJS-9), anti-mouse pErk (clone 20A), anti-mouse pAkt (Ser473) (clone M89-61), anti-mouse pS6 (clone D57.2.2E). For staining of iNKT cells, phycoerythrin (PE)-conjugated PBS-57 loaded on mouse Cd1d tetramers (mCd1d/PBS-57) were obtained from Tetramer Core Facility of the National Institute of Health.

Measurement of *in vivo* cell proliferation and ex vivo survival

Mice were given one intraperitoneal injection of 0.2 mg EdU (BD Bioscience). 12 hours after EdU injection, mice were sacrificed and organs harvested. Cells derived from the thymus were stained with antibodies specific for cell surface antigens as described above. After fixation and permeabilization, cells stained with FITC anti-EdU antibody and 7-AAD (BD Pharmingen), according to manufacturer instructions. EdU incorporation for different cell populations was measured by flow cytometry.

For the measurement of viability, we stained thymocyte suspensions with Annexin-V (BD Biosciences), 7-AAD and coupled with other surface markers Cd4, Cd8, Cd69, TCRβ, Cd25, Cd44, either *ex vivo* or 24, 48 or 72 h after *in vitro* culture in complete medium.

Cell sorting and RNA preparation

Lymphocytes were obtained from the thymus. Immune cell population including DN1-4, DP, single positive $CD4^+$ and $CD8^+$, iNKT cells were stained in combination with other cell specific markers Cd4, Cd8, Cd69, TCRβ, Cd25, Cd44 and mCd1d/PBS-57 and subsequently sorted into different subsets using a FACSAria Cell Sorter (Becton-Dickinson, San Jose, USA). Purity of sorted cell populations was over 98% as validated by flow cytometry. Sorted cells were lysed using Trizol reagent (Invitrogen) or RLT buffer from the RNeasy Micro kit (Qiagen) and RNA was extracted according to the manufacturer's instructions.

Quantitative RT-PCR

We used High capacity RNA-to-cDNA kit (applied biosystem, Carlsbad, USA) or iScript cDNA synthesis kit (BioRad) to generate cDNA for RT-PCR. PCR was carried out with a SybrGreen-based kit (FastStart Universal SYBR Green Master, Roche, Basel, Switzerland) or SensiFast SYBR No-ROX kit (Bioline) on a StepOne plus instrument (Applied biosystems, Carlsbad, USA) or a LightCycler 480 system (Roche). Primers were designed using the Roche software. We used the following primers for mouse QPCR: Zeb1 forward primer, 5'- GCCAGCAGTCATGATGAAAA-3'; Zeb1 reverse primer, 5'- TATCACAATACGGGCAGGTG-3'; Zeb2 forward primer, 5'-CCAGAGGAAACAAGGATTTCAG-3'; Zeb2 reverse primer, 5'-AGGCCTGACATG TAGTCTTGTG-3'; Gapdh forward primer, 5'-GCATGGCCTTCCGTGTTC-3'; Gapdh reverse primer, 5'- TGTCATCATACTTGGCAGGTTTCT-3'. The relative expression of Zeb1 and Zeb2 were normalized to Gapdh expression.

Western blotting

Cells were lysed in NP40 lysis buffer (20mM Tris, HCl pH7.4; 150mM NaCl; 2mM EDTA; 1% NP40) containing protease inhibitors for 30min on ice. Supernatant was collected following 10min centrifugation at 12 000g at 4°C and protein concentration was quantified by µBCA quantification kit (Thermo Fisher scientific). Fifity µg of total cellular protein from thymus were incubated during 5 minutes at 95°C. Protein samples were separated by electrophoresis using Novex 4–12% Tris-Glycine gels (Life Technologies) for 1 hour at 120V. Proteins then were transferred on a PVDF membrane (Bio-rad). After blocking with PBS 0.1% tween and 5% milk for 1 hour, membranes were probed with the following primary antibodies: anti-Gapdh (Cell Signaling Technology, 2118), anti-Zeb1 (Cell Signaling Technology, 3396, raised against a peptide around Asp846, the Cellophane mutation truncating the protein after Tyr902) over night at 4°C. Membranes were washed three times with PBS 0.1% tween, secondary antibodies were added for one hour at RT. Anti-Rabbit and anti-mouse HRP conjugate secondary antibodies were provided by Jacson Immunoresearch. Proteins were revealed with Chemiluminescence Western Lightening Plus kit (Perkin-Elmer).

RNAseq analysis

Thymic suspensions were stained in combination with anti-Cd3, anti-Cd4, anti-Cd8, anti-Cd69, anti-TCRβ and subsequently sorted into different subsets using a FACSAria Cell Sorter (Becton-Dickinson, San Jose, USA). Purity of sorted cell populations was over 98% as measured by flow cytometry. RNA libraries were prepared as previously described [60]. Briefly, total RNA was purified from $5x10^4$ sorted thymocytes using the Direct-Zol RNA microprep kit (Zymo Research) according to manufacturer instructions and was quantified using QuantiFluor RNA system (Promega). 1µl of 10µM Oligo-dT primer and 1µl of 10mM dNTPs mix were added to 0.15ng of total RNA in a final volume of 2.3µl. Oligo-dT were hybridized 3min at 72°C and reverse transcription (11 cycles) was performed. PCR pre-amplification was then conducted using 16 cycles. cDNA were purified on AmpureXP beads (Beckman Coulter) and cDNA quality was checked on D5000 screen tape and analysed on Tape station 4200 (Agilent). Three ng of cDNA were tagmented using Nextera XT DNA sample preparation kit (Illumina). Tagged fragments were further amplified and purified on AmpureXP beads (Beckman Coulter). Tagged library quality was checked on D1000 screen tape and analyzed on Tape station 4200 (Agilent). Sequencing was performed by the GenomEast platform, a member of the "France Génomique" consortium (ANR-10-INBS- 0009), on an Illumina HiSeq 4000 sequencing machine (read length 1x50nt).

Measurements of TCR signaling

Calcium response

Thymocytes were first barcoded with anti-Cd45 coupled with different fluorochromes for WT and *Cellophane* respectively and then stained at RT with fluorescent anti-Cd4 and anti-Cd8, anti-Cd69, anti-TCRβ, anti-Cd25 and anti-Cd44 antibodies, followed by a staining with Indo-1 (1µM, Life Technologies) at $1x10^7$ cells/ml for 30 min at 37°C and two times' washing at 4°C. Cells were resuspended in the RPMI medium (0.2% BSA and 25mM Hepes) and were placed at 37°C for 5-10 min prior to acquisition. Samples were acquired on a LSRII (BD) as following steps: 15 s baseline acquisition, addition of anti-Cd3 biotin (2C11, 10µg/ml), acquisition for 1 min 30 s, addition of Streptavidin (Life Technologies, 10µg/ml) and, acquisition for another 3-5 min.

Phosphorylation events

Different samples corresponding to the different mice were barcoded by labeling them with a series of anti-Cd45 antibodies coupled with different fluorochromes. For phospho-flow stainings, $3x10^6$ mixed thymocytes were stained using biotinylated Cd3 (2C11, 5µg/ml) and other surface markers for 15 min, followed by streptavidin (Life Technologies, 10µg/ml) stimulation and fixed by addition of 10 volumes of Lyse/Fix at the indicated time point. The level of pErk, pS6 or pAkt were normalized by the mean fluorescence intensity (MFI) that was detected in the non-stimulated condition (regarded as 100%) for each mouse.

***In silico* analyses**

Functional annotations of DEGs were performed using Metascape [37] or STRING [38] using default parameters. Additionally, we used several functionalities of the Immgen database browsers [29] to generate some of the figures in the supplementary information.

Statistical analysis

Statistical analyses were performed using Prism 5 (Graph-Pad Software). Two tailed unpaired t-test, paired t-test, and ANOVA tests with Bonferroni correction were used as indicated. We used the hypergeometric test and Benjamini-Hochberg p-value correction algorithm to calculate if the enrichment of the overlap between gene lists were statistically significant.

Acknowledgements

The authors acknowledge the contribution of SFR Biosciences (UMS3444/CNRS, ENSL, UCBL, US8/INSERM) facilities, in particular the Plateau de Biologie Expérimentale de la Souris, and the flow cytometry facility. We thank Bruce Beutler for sharing the *Cellophane* mutant mice. We also thank Andrew Griffiths and Kiyoto Kurima for discussions regarding *Twirler* mutant mice and Fotini Gounari and Christophe Benoist for providing RNAseq/Chipseq data of T cell development. The TW lab is supported by the Agence Nationale de la Recherche (ANR *GAMBLER* to TW and ANR JC *BaNK* to AM), the Institut National du Cancer, and receives institutional grants from the Institut National de la Santé et de la Recherche Médicale (INSERM), Centre National de la Recherche Scientifique (CNRS), Université Claude Bernard Lyon1 and ENS de Lyon, Joint Research Institute for Science and Society (JORISS). JZ is the recipient of a fellowship from the China Scholarship Council (CSC). RS and YGH were funded by a FRM grant (AJE20161236686) to YGH.

Author contributions

JZ, AB, MW, DL, DEC, ALM, AR and AM performed experiments. RS and QM performed in silico analyses. JC, LG, YGH provided reagents, conceptual insight and helped writing the paper. TW wrote the paper and supervised the work.

Conflict of interest

The authors declare no conflict of interest

Supplementary information accompanies the manuscript on *Cellular & Molecular Immunology*'s website (http://www.nature.com/cmi/)

References

1. Shah DK, Zúñiga-Pflücker JC. An Overview of the Intrathymic Intricacies of T Cell Development. *J Immunol* 2014; **192**:4017–4023.
2. Rothenberg EV, Moore JE, Yui MA. Launching the T-cell-lineage developmental programme. *Nat Rev Immunol* 2008; **8**:9–21.
3. Kurd N, Robey EA. T-cell selection in the thymus: a spatial and temporal perspective. *Immunol Rev* 2016; **271**:114–126.
4. Hogquist KA, Jameson SC. The self-obsession of T cells: how TCR signaling thresholds affect fate “decisions” and effector function. *Nat Immunol* 2014; **15**:815–823.
5. Gascoigne NRJ, Rybakin V, Acuto O, Brzostek J. TCR Signal Strength and T Cell Development. *Annu Rev Cell Dev Biol* 2016; **32**:327–348.
6. Moran AE, Holzapfel KL, Xing Y, *et al.* T cell receptor signal strength in Treg and iNKT cell development demonstrated by a novel fluorescent reporter mouse. *J Exp Med* 2011; **208**:1279–1289.
7. Godfrey DI, Uldrich AP, McCluskey J, Rossjohn J, Moody DB. The burgeoning family of unconventional T cells. *Nat Immunol* 2015; **16**:1114–1123.
8. Kronenberg M, Kinjo Y. Innate-like recognition of microbes by invariant natural killer T cells. *Curr Opin Immunol* 2009; **21**:6.
9. Tuttle KD, Krovi SH, Zhang J, *et al.* TCR signal strength controls thymic differentiation of iNKT cell subsets. *Nat Commun* 2018; **9**:2650.
10. Zhao M, Svensson MND, Venken K, *et al.* Altered thymic differentiation and modulation of arthritis by invariant NKT cells expressing mutant ZAP70. *Nat Commun* 2018; **9**:2627.
11. Malhotra N, Qi Y, Spidale NA, *et al.* SOX4 controls invariant NKT cell differentiation by tuning TCR signaling. *J Exp Med* 2018; **215**:2887–2900.
12. Ziętara N, Łyszkiewicz M, Witzlau K, *et al.* Critical role for miR-181a/b-1 in agonist selection of invariant natural killer T cells. *Proc Natl Acad Sci U S A* 2013; **110**:7407–7412.
13. Henao-Mejia J, Williams A, Goff LA, *et al.* The microRNA miR-181 is a critical cellular metabolic rheostat essential for NKT cell ontogenesis and lymphocyte development and homeostasis. *Immunity* 2013; **38**:984–997.
14. Wencker M, Turchinovich G, Di Marco Barros R, *et al.* Innate-like T cells straddle innate and adaptive immunity by altering antigen-receptor responsiveness. *Nat Immunol* 2014; **15**:80–87.
15. Seo W, Taniuchi I. Transcriptional regulation of early T-cell development in the thymus. *Eur J Immunol* 2016; **46**:531–538.
16. Maillard I, Fang T, Pear WS. Regulation of lymphoid development, differentiation, and function by the Notch pathway. *Annu Rev Immunol* 2005; **23**:945–974.
17. Murre C. Helix-loop-helix proteins and lymphocyte development. *Nat Immunol* 2005; **6**:1079–1086.
18. Hosokawa H, Rothenberg EV. Cytokines, Transcription Factors, and the Initiation of T-Cell Development. *Cold Spring Harb Perspect Biol* 2018; **10**.
19. Gheldof A, Hulpiau P, van Roy F, De Craene B, Berx G. Evolutionary functional analysis and molecular regulation of the ZEB transcription factors. *Cell Mol Life Sci CMLS* 2012; **69**:2527–2541.
20. Takagi T, Moribe H, Kondoh H, Higashi Y. DeltaEF1, a zinc finger and homeodomain transcription factor, is required for skeleton patterning in multiple

lineages. *Dev Camb Engl* 1998; **125**:21–31.
21. Caramel J, Ligier M, Puisieux A. Pleiotropic Roles for ZEB1 in Cancer. *Cancer Res* 2018; **78**:30–35.
22. Conidi A, Cazzola S, Beets K, *et al.* Few Smad proteins and many Smad-interacting proteins yield multiple functions and action modes in TGFβ/BMP signaling in vivo. *Cytokine Growth Factor Rev* 2011; **22**:287–300.
23. Scott CL, Omilusik KD. ZEBs: Novel Players in Immune Cell Development and Function. *Trends Immunol* 2019; **40**:431–446.
24. van Helden MJ, Goossens S, Daussy C, *et al.* Terminal NK cell maturation is controlled by concerted actions of T-bet and Zeb2 and is essential for melanoma rejection. *J Exp Med* 2015; **212**:2015–2025.
25. Dominguez CX, Amezquita RA, Guan T, *et al.* The transcription factors ZEB2 and T-bet cooperate to program cytotoxic T cell terminal differentiation in response to LCMV viral infection. *J Exp Med* 2015; **212**:2041–2056.
26. Omilusik KD, Best JA, Yu B, *et al.* Transcriptional repressor ZEB2 promotes terminal differentiation of CD8+ effector and memory T cell populations during infection. *J Exp Med* 2015; **212**:2027–2039.
27. Higashi Y, Moribe H, Takagi T, *et al.* Impairment of T cell development in deltaEF1 mutant mice. *J Exp Med* 1997; **185**:1467–1479.
28. Arnold CN, Pirie E, Dosenovic P, *et al.* A forward genetic screen reveals roles for Nfkbid, Zeb1, and Ruvbl2 in humoral immunity. *Proc Natl Acad Sci* 2012; **109**:12286–12293.
29. Heng TSP, Painter MW, Immunological Genome Project Consortium. The Immunological Genome Project: networks of gene expression in immune cells. *Nat Immunol* 2008; **9**:1091–1094.
30. Guan T, Dominguez CX, Amezquita RA, *et al.* ZEB1, ZEB2, and the miR-200 family form a counterregulatory network to regulate CD8+ T cell fates. *J Exp Med* 2018; **215**:1153–1168.
31. Jones ME, Zhuang Y. Stage-specific functions of E-proteins at the β-selection and T-cell receptor checkpoints during thymocyte development. *Immunol Res* 2011; **49**:202–215.
32. Emmanuel AO, Arnovitz S, Haghi L, *et al.* TCF-1 and HEB cooperate to establish the epigenetic and transcription profiles of CD4+CD8+ thymocytes. *Nat Immunol* 2018; **19**:1366–1378.
33. Rahim MMA, Tu MM, Mahmoud AB, *et al.* Ly49 Receptors: Innate and Adaptive Immune Paradigms. *Front Immunol* 2014; **5**.
34. Grigoriadou K, Boucontet L, Pereira P. Most IL-4-producing gamma delta thymocytes of adult mice originate from fetal precursors. *J Immunol Baltim Md 1950* 2003; **171**:2413–2420.
35. Gapin L. iNKT cell autoreactivity: what is “self” and how is it recognized? *Nat Rev Immunol* 2010; **10**:272–277.
36. Tuttle KD, Gapin L. Characterization of Thymic Development of Natural Killer T Cell Subsets by Multiparameter Flow Cytometry. *Methods Mol Biol Clifton NJ* 2018; **1799**:121–133.
37. Zhou Y, Zhou B, Pache L, *et al.* Metascape provides a biologist-oriented resource for the analysis of systems-level datasets. *Nat Commun* 2019; **10**:1523.
38. Szklarczyk D, Franceschini A, Wyder S, *et al.* STRING v10: protein-protein interaction networks, integrated over the tree of life. *Nucleic Acids Res* 2015; **43**:D447-452.
39. Liston A, Hardy K, Pittelkow Y, *et al.* Impairment of organ-specific T cell negative

779 selection by diabetes susceptibility genes: genomic analysis by mRNA profiling.
780 *Genome Biol* 2007; **8**:R12.
781 40. Kastner P, Chan S, Vogel WK, *et al.* Bcl11b represses a mature T-cell gene
782 expression program in immature CD4(+)CD8(+) thymocytes. *Eur J Immunol* 2010;
783 **40**:2143–2154.
784 41. Yoshida H, Lareau CA, Ramirez RN, *et al.* The cis-Regulatory Atlas of the Mouse
785 Immune System. *Cell* 2019; **176**:897-912.e20.
786 42. Bedel R, Berry R, Mallevaey T, *et al.* Effective functional maturation of invariant
787 natural killer T cells is constrained by negative selection and T-cell antigen receptor
788 affinity. *Proc Natl Acad Sci* 2014; **111**:E119–E128.
789 43. Hayes SM, Love PE. Strength of signal: a fundamental mechanism for cell fate
790 specification. *Immunol Rev* 2006; **209**:170–175.
791 44. Haks MC, Lefebvre JM, Lauritsen JPH, *et al.* Attenuation of gammadeltaTCR
792 signaling efficiently diverts thymocytes to the alphabeta lineage. *Immunity* 2005;
793 **22**:595–606.
794 45. Alonzo ES, Gottschalk RA, Das J, *et al.* Development of promyelocytic zinc finger
795 and ThPOK-expressing innate gamma delta T cells is controlled by strength of TCR
796 signaling and Id3. *J Immunol Baltim Md 1950* 2010; **184**:1268–1279.
797 46. Ilangumaran S, Forand-Boulerice M, Bousquet SM, *et al.* Loss of GIMAP5
798 (GTPase of immunity-associated nucleotide binding protein 5) impairs calcium
799 signaling in rat T lymphocytes. *Mol Immunol* 2009; **46**:1256–1259.
800 47. Howie D, Nolan KF, Daley S, *et al.* MS4A4B is a GITR-associated membrane
801 adapter, expressed by regulatory T cells, which modulates T cell activation. *J*
802 *Immunol Baltim Md 1950* 2009; **183**:4197–4204.
803 48. Carlson CM, Endrizzi BT, Wu J, *et al.* Kruppel-like factor 2 regulates thymocyte
804 and T-cell migration. *Nature* 2006; **442**:299–302.
805 49. Gubbels Bupp MR, Edwards B, Guo C, *et al.* T cells require Foxo1 to populate
806 the peripheral lymphoid organs. *Eur J Immunol* 2009; **39**:2991–2999.
807 50. Li L, Bhatia R. Molecular Pathways: Stem Cell Quiescence. *Clin Cancer Res Off*
808 *J Am Assoc Cancer Res* 2011; **17**:4936–4941.
809 51. Hedrick SM, Michelini RH, Doedens AL, Goldrath AW, Stone EL. FOXO
810 transcription factors throughout T cell biology. *Nat Publ Group* 2012; **12**:649–662.
811 52. Shi LZ, Saravia J, Zeng H, *et al.* Gfi1-Foxo1 axis controls the fidelity of effector
812 gene expression and developmental maturation of thymocytes. *Proc Natl Acad Sci U*
813 *S A* 2017; **114**:E67–E74.
814 53. D'Cruz LM, Knell J, Fujimoto JK, Goldrath AW. An essential role for the
815 transcription factor HEB in thymocyte survival, Tcra rearrangement and the
816 development of natural killer T cells. *Nat Immunol* 2010; **11**:240–249.
817 54. Brabletz T, Jung A, Hlubek F, *et al.* Negative regulation of CD4 expression in T
818 cells by the transcriptional repressor ZEB. *Int Immunol* 1999; **11**:1701–1708.
819 55. Postigo AA, Ward E, Skeath JB, Dean DC. zfh-1, the Drosophila Homologue of
820 ZEB, Is a Transcriptional Repressor That Regulates Somatic Myogenesis. *Mol Cell*
821 *Biol* 1999; **19**:7255–7263.
822 56. Grégoire JM, Roméo PH. T-cell expression of the human GATA-3 gene is
823 regulated by a non-lineage-specific silencer. *J Biol Chem* 1999; **274**:6567–6578.
824 57. Wang L, Ni X, Covington KR, *et al.* Genomic profiling of Sézary syndrome
825 identifies alterations of key T cell signaling and differentiation genes. *Nat Genet*
826 2015; **47**:1426–1434.
827 58. Mishra A, La Perle K, Kwiatkowski S, *et al.* Mechanism, Consequences, and
828 Therapeutic Targeting of Abnormal IL15 Signaling in Cutaneous T-cell Lymphoma.

Cancer Discov 2016; **6**:986–1005.
59. Doisne J-M, Bartholin L, Yan K-P, *et al.* iNKT cell development is orchestrated by different branches of TGF- signaling. *J Exp Med* 2009; **206**:1365–1378.
60. Picelli S, Faridani OR, Björklund AK, Winberg G, Sagasser S, Sandberg R. Full-length RNA-seq from single cells using Smart-seq2. *Nat Protoc* 2014; **9**:171–181.

Figure legends

Figure 1: Zeb1 expression in WT and *Cellophane* thymocytes

(A-B) RT-PCR analysis of RNA from sorted thymocyte subsets isolated from C57BL/6 mice, as indicated. Results are presented relative to expression of the control gene *Gapdh*. (C) WB analysis of Zeb1 expression in total thymocytes of WT and *Cellophane* mice, as indicated. Data are representative of three independent experiments with 3 to 6 mice (A-B) or three independent experiments with three mice (C).

Figure 2: Cellularity and proportion of T cell subsets in *Cellophane* mice.

(A) Total cell number from the thymus, spleen, liver and LN. (B) Percentages and absolute numbers of indicated T cell subsets (DN, DP, Cd4 SP and Cd8 SP) in the thymus. (C) Percentages and absolute numbers of indicated DN subsets defined by Cd44 and Cd25 expression in the thymus. (D-E) Percentages and absolute numbers of (D) Cd4 T cells and (E) Cd8 T cells. (F) Percentages and absolute numbers of $CD8^+$ $Cd44^+$ memory T cell in LN and spleen. Each dot represents an individual mouse. Data are pooled from 7 to 8 mice in four experiments (A-E) or 3 to 6 mice in two experiments (F). The statistical analysis was performed using unpaired Student *t* test.

Figure 3: *Cellophane* mice have decreased numbers of thymic DP and lack iNKT cells, $NK1.1^+$ γδ T cells and $Ly49^+$ Cd8 cells.

(A) Flow cytometry analysis of Cd1d-tet^+ iNKT cells (black gate) from thymus, spleen, and liver in wild-type (WT) and *Cellophane* (Cello) homozygous mice as indicated. (B) Percentage and absolute numbers of iNKT cells (mCd1d/PBS-57^+ $TCR\beta^+$) in thymus, spleen, and liver. (C) Flow cytometry analysis of $NK1.1^-$ and $NK1.1^+$ γδ T cells (black square gates) from the spleen of WT and *Cellophane* mice. (D) Percentage within total γδ T cells and absolute numbers of $NK1.1^-$ and $NK1.1^+$ γδ T cells in spleen and LN. (E) Percentage within total thymic iNKT of stages 0-3, as defined by Cd24, Cd44 and NK1.1 expression. (F) Flow cytometry analysis of $Cd8^+$ $Cd44^+$ $Ly49A^+$ / $Ly49F^+$ / $Ly49G2^+$ T cells (black square gates) from LN and spleen in WT and *Cellophane* mice. (G) Percentage within $Cd8^+Cd44^+$ T cells and absolute numbers of $Cd8^+$ $Cd44^+$ $Ly49^+$ T cells in spleen and LN. Each dot represents an

individual mouse. Data are representative of 2-4 independent experiments with 6 mice in total for each panel. The statistical analysis was performed using unpaired Student *t* test.

Figure 4: The role of Zeb1 in T cell development is cell-intrinsic.

(A) Flow cytometry analysis of the indicated thymocyte subsets from BM chimeras. Frequencies are shown for each subset. Recipients were Ly5a mice (Cd45.1), and donor BM was either from Ly5a x C57BL/6 (Cd45.1/2) or *Cellophane* (Cd45.2). (B) iNKT cell and (C) $Cd8^+$ $Ly49^+$ T cell frequencies in the spleen, liver or LN from the same BM chimera described in *A*. (D) DN1-4, DP, Cd4+ and Cd8+ cell reconstitution in thymus of competitive BM chimeras. Recipients were Ly5a mice (Cd45.1) and donor BM was a 1:1 mix of Ly5a x C57BL/6 (Cd45.1/2) and *Cellophane* (Cd45.2). 8 weeks after BM transplantation, cells were analyzed by flow cytometry. The number above the red bar shows the percentage of indicated cells originating from the *Cellophane* BM. (E-F) Frequency of iNKT cells (E) and $Ly49^+$ cells within $Cd8^+$ $Cd44^+$ T cells in spleen, liver or LN from BM chimera described in *D*. Each dot represents an individual mouse. Results show the pooled data from two to three independent experiments for a total of 2 to 6 mice per group in each panel. Statistical analyses were performed using unpaired Student *t* test.

Figure 5: *Cellophane* DP cells have reduced survival and proliferation.

(A) Percentages of Annexin V-negative cells (live cells) by wild-type and *Cellophane* thymocytes cultured for 0-72h. Each graph shows a different subset, as indicated (B) EdU incorporation of wild-type and *Cellophane* thymocytes after a 12-hour *in vivo* pulse of 0.2 mg EdU. (C) Frequencies of Ki67+ cells in DN1-4 subsets from WT and *Cellophane* mice. (D) Ki67 nuclear staining in DP thymocytes from WT and *Cellophane* mice. Bar graphs (right panel) show mean+/-SD fluorescence intensity (MFI). Each dot represents an individual mouse. Data are pooled from three independent experiments with three mice in each group (A-D). Statistical analysis was performed using unpaired Student *t* test.

Figure 6: *Cellophane* DP thymocytes display increased TCR signaling.

(A) Flow cytometry analysis of Cd69, Cd25, Cd5, Nur77, Cd4, Cd8 and Tcrβ expression (mean fluorescence intensity) in DP thymocytes of wild-type and *Cellophane* mice. (B) Left panels: Representative flow cytometry analysis of iNKT1 (Plzf lo, Rorγt-, Tbet+), iNKT2 (Plzf hi, Rorγt-, Tbet-), and iNKT17 (Plzf int, Rorγt+, Tbet-) subsets in wild-type and *Cellophane* mice (as defined by the gating strategy shown in the upper-panel). Right panel: graphs of the percentage of iNKT subsets within total iNKT. (C) The TCRVβ repertoire of thymic iNKT cells was analyzed by flow cytometry. Bar graphs show mean+/-SD frequencies of individual Vβ chain within iNKT cells. (D) Expression of Cd4, Tbet, Egr2 and Plzf in iNKT cells as measured by flow cytometry (mean fluorescence intensity). (E) Phosphorylation levels of Erk, S6 and Akt (S473) in resting DP thymocytes from WT and *Cellophane* mice. (F) Phosphorylation levels of Erk, S6 and Akt (Ser473) in DP cells stimulated with anti-Cd3 antibody for the indicated time. Results are normalized to the non-stimulated condition (ie basal level, 100%) for each group. (G) Representative histogram overlay showing the Ca^{2+} flux in thymic DP cells from wild-type or *Cellophane* mice stimulated with anti-Cd3 antibodies, as measured by flow cytometry. Thymocytes were activated following incubation with biotinylated anti-Cd3 (Arrow) followed by cross-linking with streptavidin (Arrowhead). (H) Dot plots showing the AUC (Area under curve) and Ca^{2+} peak. Statistical analysis was performed using unpaired Student *t* test. Each dot represents an individual mouse. Data are pooled from three experiments with a total of 8 mice in each group (A) or three experiments with 6 mice (B), or three mice (C), or two experiments with 6 mice (D-F) or three experiments with 3 mice (G-H).

Figure 7: RNAseq analysis of *Zeb1*-regulated genes. (A)Volcano-plot representing -log10 (adjusted p-value) as a function of the estimated log2 fold-change. Significant genes were selected using the following thresholds: adjusted p-value lower than 0.05 and absolute value of log2 Fold-Change greater than 1. For significant genes (plotted in red), a selection of gene names is displayed. Results are representative of biological replicates in each group. (B) Flow cytometry analysis of several genes identified by RNA-seq either up-regulated (Foxo1, Ms4a4b, integrin α4:β7, Ccr7, Ccr4, Cd74, Cd53,) or downregulated (Cd81) in *Cellophane*. Data are pooled from two independent experiments with a total of 6 mice. (C) Expression level of two

selected gene list (200 genes for each list) - either upregulated (WT<Cello) or downregulated (WT>Cello) in *Cellophane* with fold change>2 and p-value<0.05 - in different αβ T cell subsets, as indicated. Graphs are adapted from the Immgen website. (D) Pathway analysis of DEGs in (A) using Metascape. Selected terms are shown among the most significant ones. (E) Venn diagram showing the overlap between DEGs in (A) and genes located in the 100kb around OCRs containing Zeb1 motifs, and for which chromatin accessibility changed during T cell development (corresponding clusters can be visualized in Figure S4B). The genes upregulated in WT are shown in red while the downregulated are shown in blue.

Supplementary figure legends

Table S1: Genes differentially expressed between control and *Cellophane* DP. Filters: Adjusted p-value<0.05, Fold change>2.

Table S2: Pathway analysis of genes up regulated or down regulated in *Cellophane* DP compared to control DP, using "metascape".

Table S3: Functional annotation of genes up regulated in *Cellophane* DP compared to control DP. Individual Pubmed queries were performed to search for association between corresponding genes and T cell activation or T cell development. A summary of the association and the reference of the article are provided.

Table S4: Functional annotation of genes up regulated in *Cellophane* DP compared to control DP using the Pubmed module search in "String".

Figure S1: *Zeb1* is highly expressed in DP and co-regulated with *Tcf12*.
(A) Expression profile of Zeb1 and Zeb2 mRNA level in thymic αβ T cell subsets. Image is adapted from Immgen (http://www.immgen.org/). The red color indicates higher expression. (B) Genes for which the expression pattern in αβ T cell subsets is highly correlated with that of Zeb1. The figure is adapted from data on the Immgen browser (http://www.immgen.org/).

Figure S2: Decreased numbers of thymocyte subsets and peripheral NKT cells in *Cellophane*→Ly5a BM chimeric mice
Cell numbers calculated for the panels A-C in Figure 4, as indicated.

Figure S3: **The role of Zeb1 in T cell development is cell-intrinsic**. (A-C) Flow cytometry analysis of indicated thymocyte subsets or thymus/liver NKT cells from BM chimeras. Recipients were C57BL/6 (WT) mice or *Cellophane*, as indicated, and donor BM was either Ly5a x C57BL/6 (WT) or *Cellophane,* as indicated. Graphs show the mean+/-SD frequency or number of 3-4 mice in 2 experiments. (D) Mixed BM chimeric mice described in Figure 4D were analyzed by flow cytometry for the

985 indicated subsets. Results show the BM donor origin in percentage for each gated
986 subset. Mean +/-SD of 6 mice.
987
988 **Figure S4**: **Zeb1 regulates epigenetic remodeling during T cell development**. (A)
989 Snapshot of Figure 5 in Yoshida et al [41], highlighting the cluster of transcription
990 factors predicted to regulate chromatin accessibility during T cell development. (B)
991 Boxplot graphs showing the mean accessibility of different open chromatin regions
992 (OCRs), as determined by ATACseq by Yoshida *et al*, in developing T cell subsets,
993 as indicated. All OCRs contain Zeb1 binding sites.

Figure 1

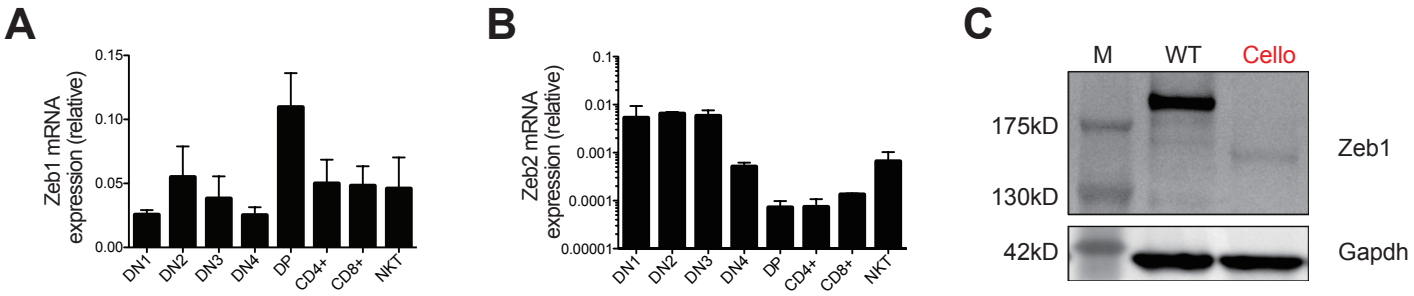
A
Zeb1 mRNA expression (relative)
0.15
0.10
0.05
0.00
DN1
DN2
DN3
DN4
DP
CD4+
CD8+
NKT
B
Zeb2 mRNA expression (relative)
0.1
0.01
0.001
0.0001
0.00001
DN1
DN2
DN3
DN4
DP
CD4+
CD8+
NKT
C
M
WT
Cello
175kD
130kD
Zeb1
42kD
Gapdh

Figure 2

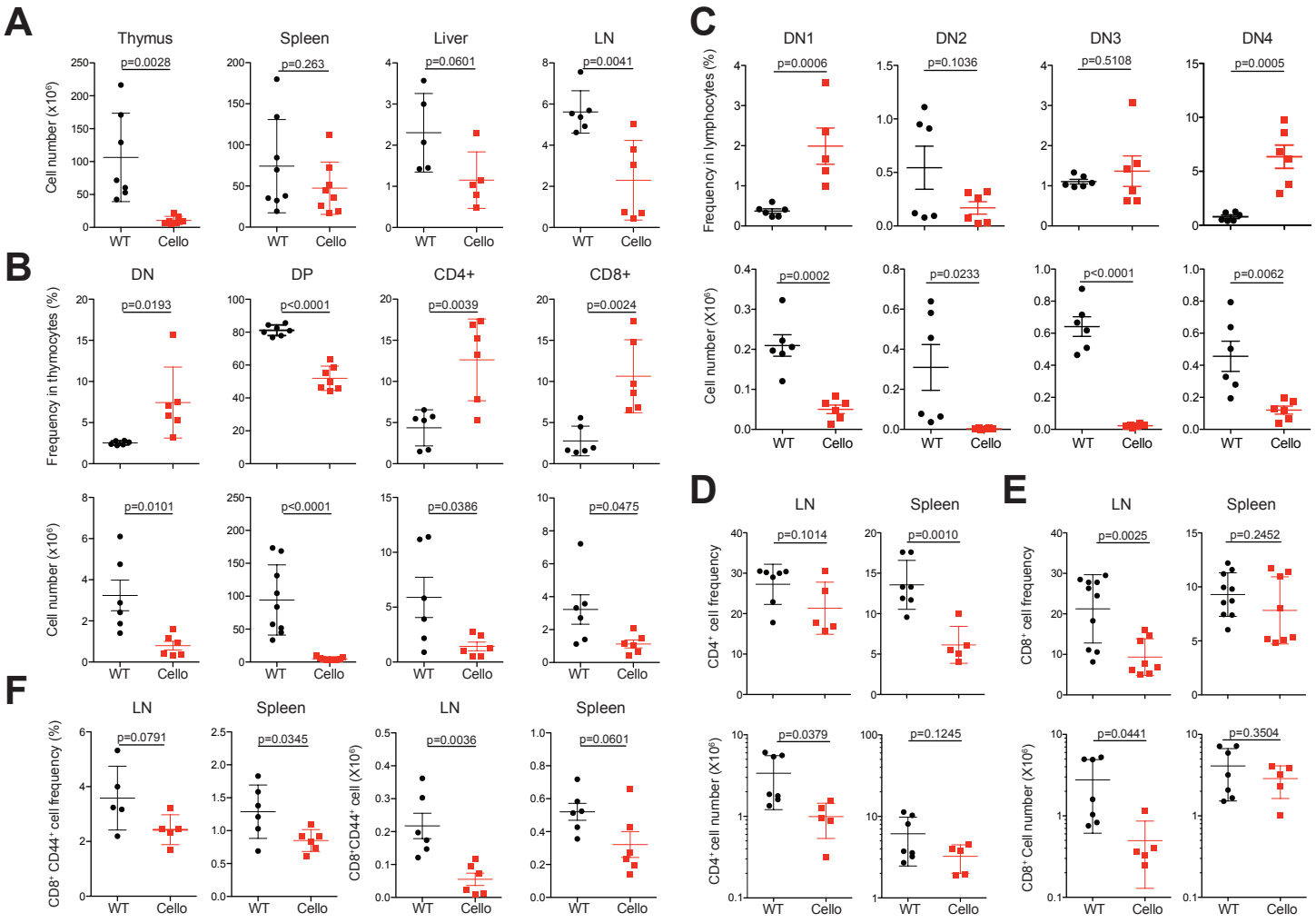
A
Thymus
Spleen
Liver
LN
Cell number (x10⁶)
p=0.0028
p=0.263
p=0.0601
p=0.0041
WT
Cello
B
DN
DP
CD4+
CD8+
Frequency in thymocytes (%)
p=0.0193
p<0.0001
p=0.0039
p=0.0024
Cell number (x10⁶)
p=0.0101
p<0.0001
p=0.0386
p=0.0475
C
DN1
DN2
DN3
DN4
Frequency in lymphocytes (%)
p=0.0006
p=0.1036
p=0.5108
p=0.0005
Cell number (X10⁶)
p=0.0002
p=0.0233
p<0.0001
p=0.0062
D
LN
Spleen
CD4⁺ cell frequency
p=0.1014
p=0.0010
CD4⁺ cell number (X10⁶)
p=0.0379
p=0.1245
E
LN
Spleen
CD8⁺ cell frequency
p=0.0025
p=0.2452
CD8⁺ Cell number (X10⁶)
p=0.0441
p=0.3504
F
LN
Spleen
LN
Spleen
CD8⁺ CD44⁺ cell frequency (%)
p=0.0791
p=0.0345
CD8⁺CD44⁺ cell (X10⁶)
p=0.0036
p=0.0601

Figure 3

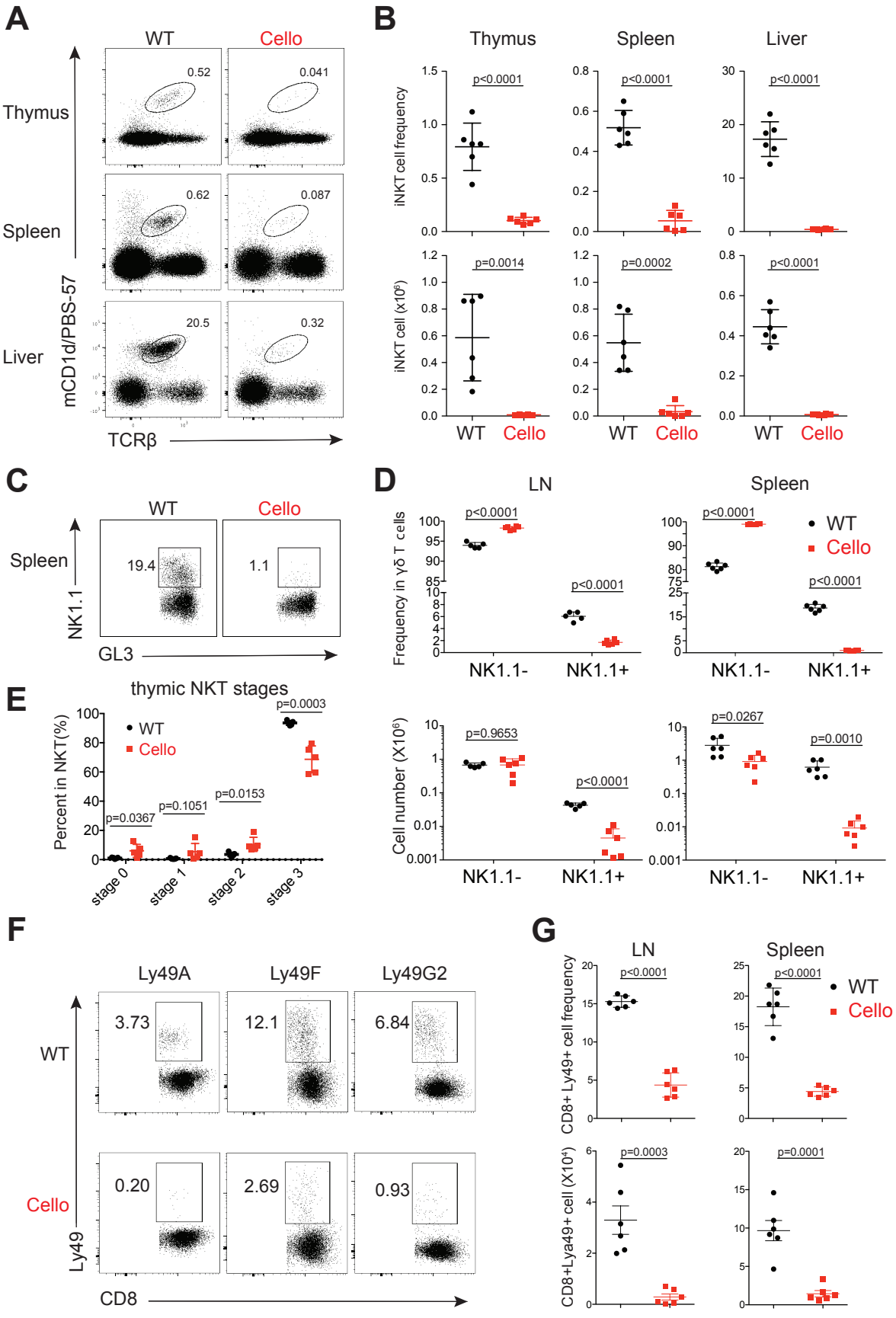
A
WT
Cello
Thymus
Spleen
Liver
0.52
0.041
0.62
0.087
20.5
0.32
mCD1d/PBS-57
TCRβ
B
Thymus
Spleen
Liver
iNKT cell frequency
iNKT cell (x10⁶)
p<0.0001
p=0.0014
p=0.0002
WT
Cello
C
Spleen
NK1.1
GL3
19.4
1.1
D
LN
Spleen
Frequency in γδ T cells
Cell number (X10⁶)
p<0.0001
p=0.9653
p=0.0267
p=0.0010
NK1.1-
NK1.1+
E
thymic NKT stages
Percent in NKT(%)
p=0.0003
p=0.0367
p=0.1051
p=0.0153
stage 0
stage 1
stage 2
stage 3
F
Ly49A
Ly49F
Ly49G2
3.73
12.1
6.84
0.20
2.69
0.93
Ly49
CD8
G
CD8+ Ly49+ cell frequency
CD8+Ly49+ cell (X10⁴)
p=0.0003
p=0.0001

Figure 4

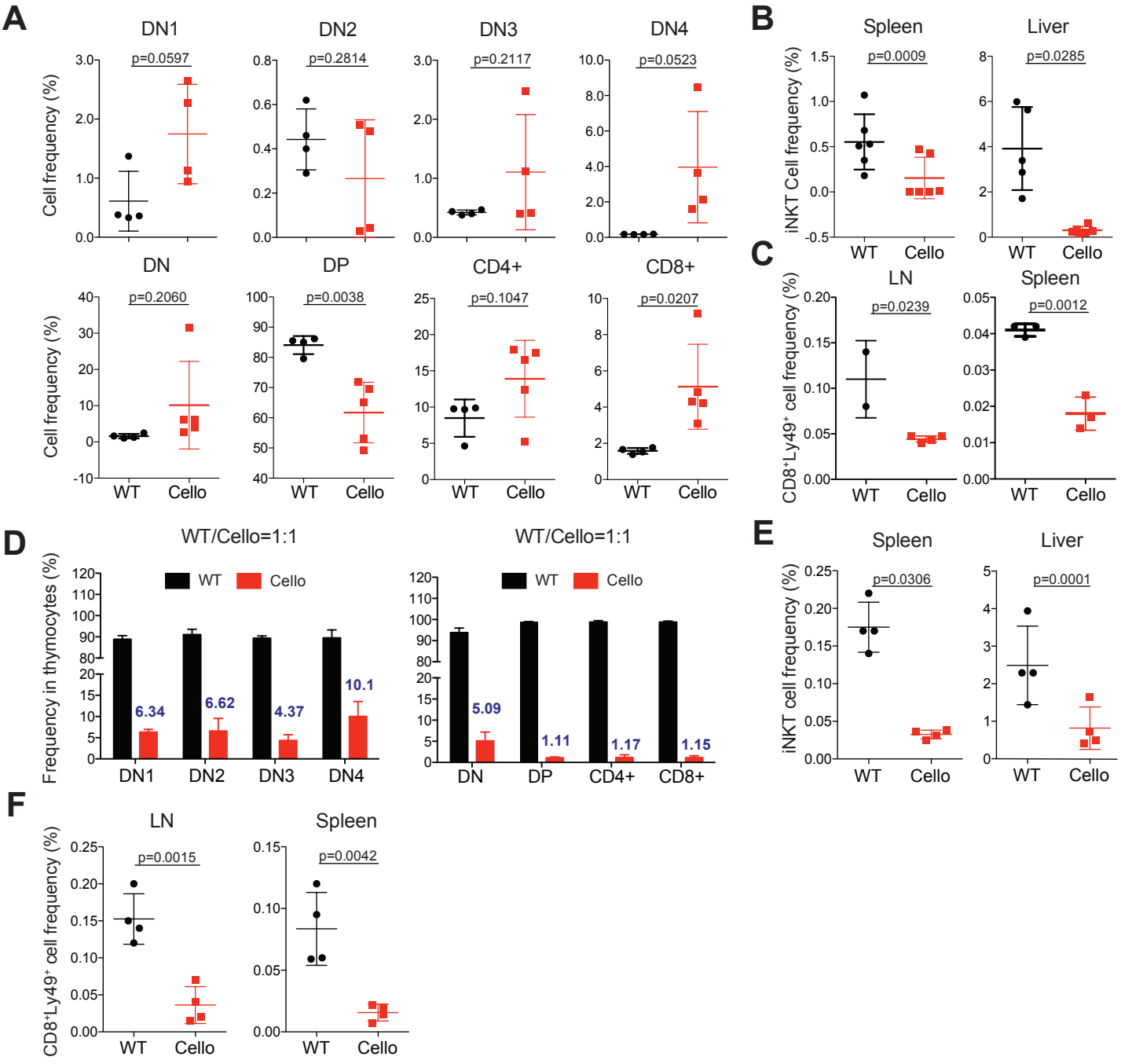
A
DN1
DN2
DN3
DN4
Cell frequency (%)
p=0.0597
p=0.2814
p=0.2117
p=0.0523
DN
DP
CD4+
CD8+
p=0.2060
p=0.0038
p=0.1047
p=0.0207
WT
Cello
B
Spleen
Liver
iNKT Cell frequency (%)
p=0.0009
p=0.0285
C
LN
Spleen
CD8+Ly49+ cell frequency (%)
p=0.0239
p=0.0012
D
WT/Cello=1:1
Frequency in thymocytes (%)
6.34
6.62
4.37
10.1
5.09
1.11
1.17
1.15
DN1
DN2
DN3
DN4
DN
DP
CD4+
CD8+
E
iNKT cell frequency (%)
p=0.0306
p=0.0001
F
p=0.0015
p=0.0042

Figure 5

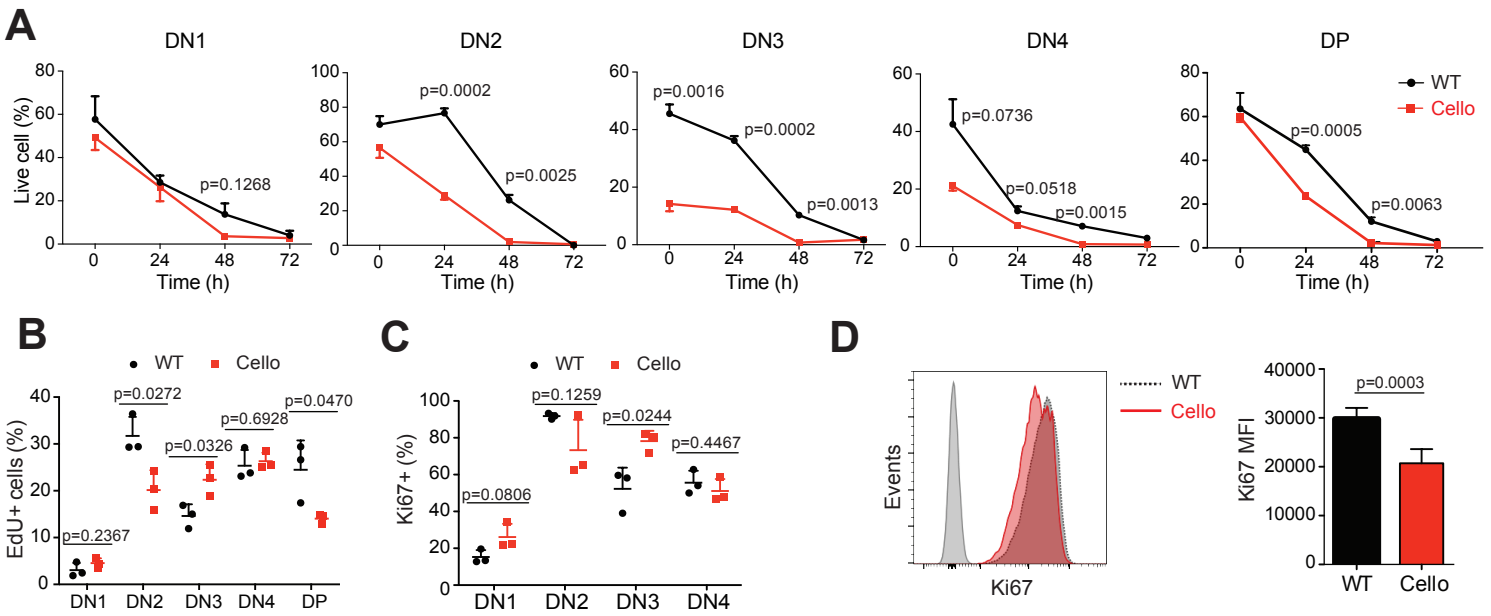
A
DN1
DN2
DN3
DN4
DP
Live cell (%)
Time (h)
p=0.1268
p=0.0002
p=0.0025
p=0.0016
p=0.0002
p=0.0013
p=0.0736
p=0.0518
p=0.0015
p=0.0005
p=0.0063
WT
Cello
B
EdU+ cells (%)
p=0.2367
p=0.0272
p=0.0326
p=0.6928
p=0.0470
C
Ki67+ (%)
p=0.0806
p=0.1259
p=0.0244
p=0.4467
D
Events
Ki67
Ki67 MFI
p=0.0003

Figure 6

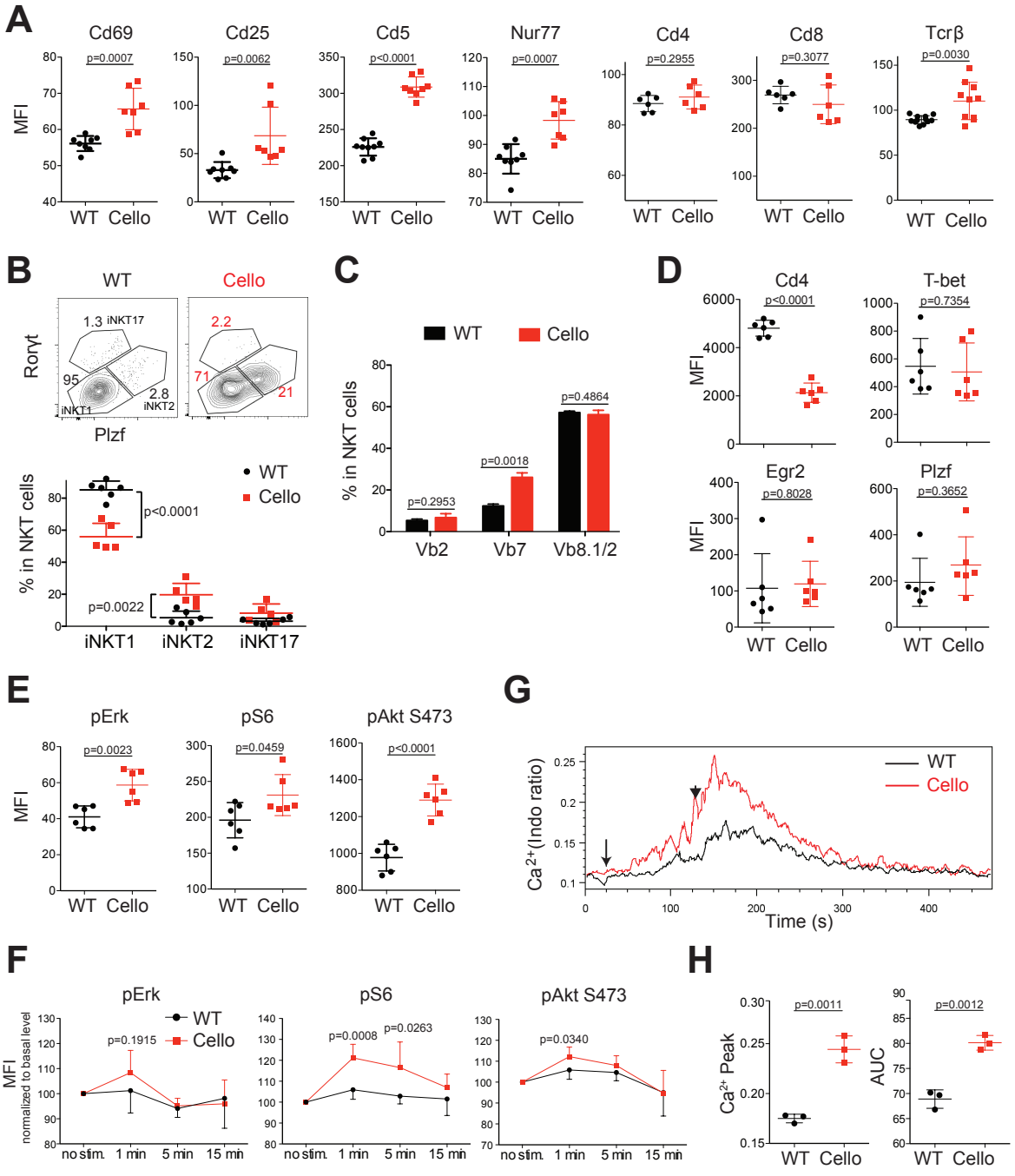
A
Cd69
Cd25
Cd5
Nur77
Cd4
Cd8
Tcrβ
MFI
p=0.0007
p=0.0062
p<0.0001
p=0.0007
p=0.2955
p=0.3077
p=0.0030
WT Cello
B
WT
Cello
Rorγt
Plzf
1.3 iNKT17
95
2.8
iNKT1
iNKT2
2.2
71
21
% in NKT cells
p<0.0001
p=0.0022
iNKT1
iNKT2
iNKT17
C
WT
Cello
% in NKT cells
p=0.2953
p=0.0018
p=0.4864
Vb2
Vb7
Vb8.1/2
D
Cd4
T-bet
Egr2
Plzf
MFI
p<0.0001
p=0.7354
p=0.8028
p=0.3652
E
pErk
pS6
pAkt S473
p=0.0023
p=0.0459
p<0.0001
F
pErk
pS6
pAkt S473
MFI
normalized to basal level
p=0.1915
p=0.0008
p=0.0263
p=0.0340
no stim.
1 min
5 min
15 min
G
Ca2+(Indo ratio)
Time (s)
H
Ca2+ Peak
AUC
p=0.0011
p=0.0012

Figure 7

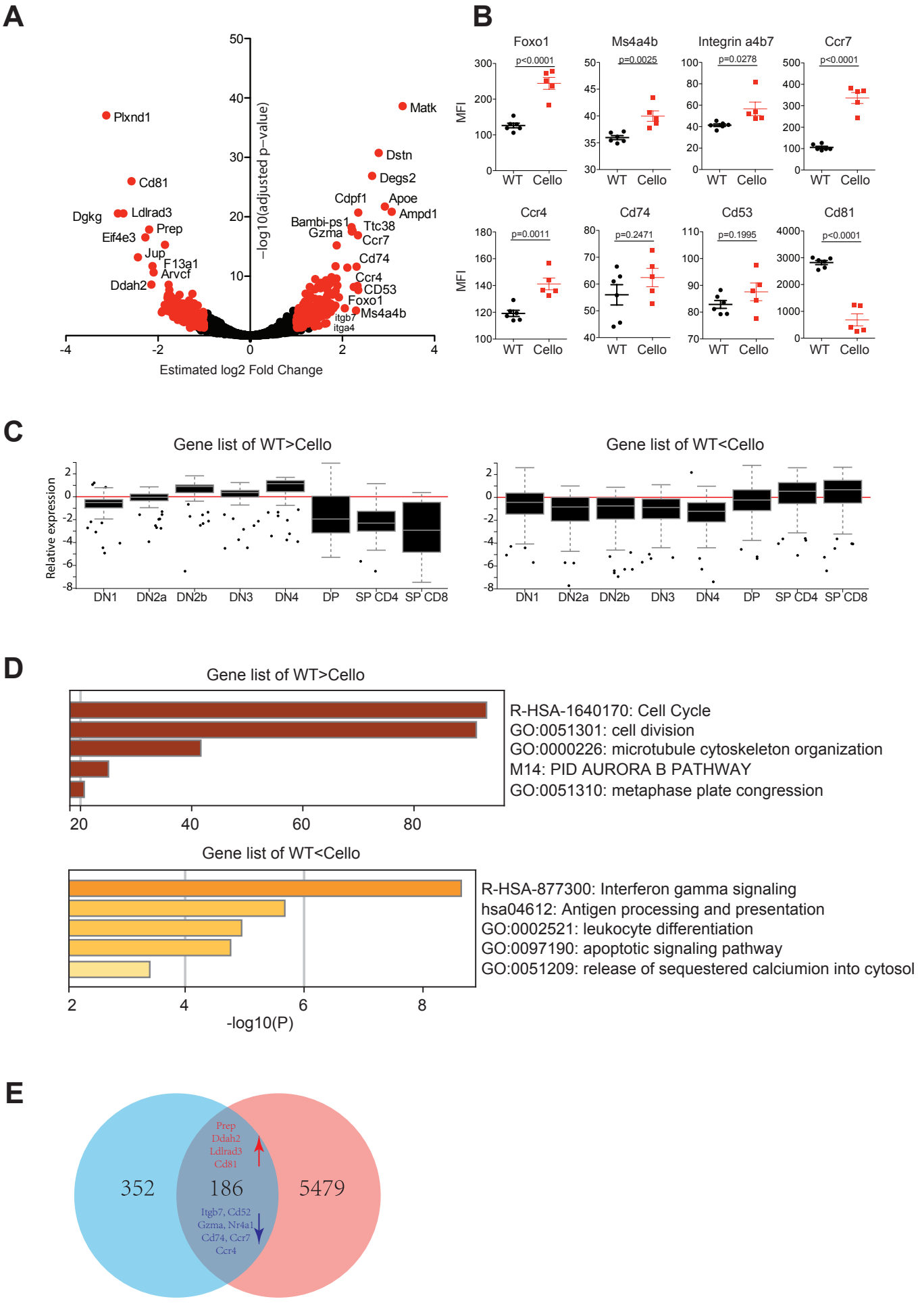
A
Plxnd1
Cd81
Dgkg
Ldlrad3
Prep
Eif4e3
Jup
F13a1
Arvcf
Ddah2
Matk
Dstn
Degs2
Cdpf1
Apoe
Ampd1
Bambi-ps1
Ttc38
Gzma
Ccr7
Cd74
Ccr4
CD53
Foxo1
Ms4a4b
itgb7
itga4
−log10(adjusted p−value)
Estimated log2 Fold Change
B
Foxo1
Ms4a4b
Integrin a4b7
Ccr7
Ccr4
Cd74
Cd53
Cd81
MFI
WT
Cello
C
Gene list of WT>Cello
Gene list of WT<Cello
Relative expression
DN1
DN2a
DN2b
DN3
DN4
DP
SP CD4
SP CD8
D
Gene list of WT>Cello
R-HSA-1640170: Cell Cycle
GO:0051301: cell division
GO:0000226: microtubule cytoskeleton organization
M14: PID AURORA B PATHWAY
GO:0051310: metaphase plate congression
Gene list of WT<Cello
R-HSA-877300: Interferon gamma signaling
hsa04612: Antigen processing and presentation
GO:0002521: leukocyte differentiation
GO:0097190: apoptotic signaling pathway
GO:0051209: release of sequestered calciumion into cytosol
-log10(P)
E
352
186
5479
Prep
Ddah2
Ldlrad3
Cd81
Itgb7, Cd52
Gzma, Nr4a1
Cd74, Ccr7
Ccr4